ELSEVIER

www.elsevier.nl/locate/ica

Inorganica Chimica Acta 312 (2001) 81–87

Inorganica Chimica Acta

Synthesis and characterization of square planar nickel(II) complexes with *p*-fluorobenzaldehyde thiosemicarbazone derivatives

Marisa Belicchi Ferrari [a,*], Silvia Capacchi [b], Franco Bisceglie [a], Giorgio Pelosi [a], Pieralberto Tarasconi [a]

[a] *Dipartimento di Chimica Generale ed Inorganica, Chimica Analitica, Chimica Fisica, Università di Parma, Viale delle Scienze, I-43100 Parma, Italy*

[b] *C.I.R.C.M.S.B., Unità di Ricerca di Parma, Parma, Italy*

Received 17 June 2000; accepted 2 October 2000

Abstract

New thiosemicarbazone nickel complexes (**1**–**7**), derived from *p*-fluorobenzaldehyde and differently substituted thiosemicarbazides, were synthetized and characterized by means of NMR and IR techniques. The *p*-fluorobenzaldehyde 4-ethylthiosemicarbazone Et-Hfbt (**1**) and its complex [Ni(Et-fbt)$_2$] (**2**) were also characterized by X-ray diffractometry. Molecule **1** consists of two units: the *p*-fluorobenzaldehyde residue and the thiosemicarbazonic chain. In the reaction of **1** with $NiAc_2{\cdot}4H_2O$, complex **2** was afforded. The molecular structure of **2** consists of the neutral complexes [Ni(Et-fbt)$_2$] with the metal not lying on a symmetry centre, with two consequently independent ligand molecules; the coordination results in a square planar geometry slightly twisted towards a tetrahedron, involving the sulfur and the hydrazine nitrogen atoms of the two ligands in a *trans* configuration.

Keywords: Thiosemicarbazone nickel complexes; Crystal structures; NMR spectra

1. Introduction

The discovery and the development of new, more effective cancer medicines is one of the main goals of present day medicine and chemical investigations. Recently, the discovery of the antitumor effects of inorganic and particularly of metal complexes and their use to cure cancer diseases have received increasing attention. Metal chelation is a very important process, useful both to remove a toxic metal from a polluted environment and to afford new chemical features to metal complexes in order to make them suitable for practical purposes (for instance pharmacological applications).

On the basis of these observations, we had previously synthesized and characterized polyfunctional organic molecules, belonging to the class of thiosemicabazones, able to behave as chelate ligands towards metal centres, and their non-cisplatin-like complexes.

In particular, copper(II) complexes, containing aromatic thiosemicarbazones of important biological intermediates (pyridoxal or 5-formyluracil thiosemicarbazone) determined the *apoptosis* process on human leukemic cell lines [1]. These ligands, in their neutral or deprotonated form, behaved as a SNO terdentate chelate towards metal ions essential for life. Now we have prepared new nickel complexes bearing the lipophilic *p*-fluorobenzene group and differently N(4)-substituted thiosemicarbazides (Fig. 1), in order to verify whether SN monodeprotonable ligands are able to condition the complicated mechanisms ruling the self-regulated cell death on the same human cell lines U937 taken as a model [2].

* Corresponding author. Fax: +39-0521-905 557.
E-mail address: chimic8@ipruniv.cce.unipr.it (M.B. Ferrari).

0020-1693/01/$ - see front matter
PII: S0020-1693(00)00339-X

Nickel has been chosen since its trace presence is now recognized to be essential for bacteria, plants, animals and humans [3], and it is also known that many nickel complexes, coordinatively unsaturated, can behave as Lewis acids. Having free coordinative positions around the metal ion in our products with the nickel(II) in a *trans* square planar SN configuration, our compounds (all structurally similar) have been studied to widen our comprehension of the role played by the metal and to find out structural criteria for nickel complexes to be biologically effective.

This screening method is appropriate for the antitumor drugs whose pharmacopoeia is still lacking, but unfortunately our molecules, though soluble and stable in DMSO solutions, precipitated when brought into contact with the biological medium, giving unreproducible results and did not allow a structure–activity correlation. However it is remarkable to notice that among the several nickel complexes structurally known and reported in literature only four of them, containing SN bidentate thiosemicarbazones, presented a *trans* square planar coordination [4] analogous to that found in our complexes, where the nickel ion lies in the field of the S_2N_2 chromophore.

2. Experimental

All materials and solvents were obtained from commercial suppliers and used without further purification. *p*-Fluorobenzaldehyde was from Sigma, and thiosemicarbazide and its derivatives were from Janssen. ^{1}H NMR were obtained at room temperature (r.t.) on a Brucker AMX-300 spectrometer, and chemical shifts are given in units of δ relative to TMS as an internal reference. For all compounds, dissolved in DMSO-d_6, the two signals of DMSO and water arose at 2.5 and 3.4 ppm, respectively. Infrared (IR) spectra were recorded on a Nicolet 5PCFT-IR spectrophotometer in the frequency range 4000–400 cm^{-1}. CI-MS (m/z, 70 eV) were obtained on a Finnegan 1020 6c mass spectrometer. Elemental analyses were performed by the Microanalytical Laboratory of the University of Parma (Dipartimento di Chimica Generale ed Inorganica).

2.1. Synthesis of the *p*-fluorobenzaldehyde N^4-ethylthiosemicarbazone Et-Hfbt (**1**)

To a solution of 4-ethylthiosemicarbazide (0.151 g, 1.27×10^{-3} mol) in 10 ml of EtOH 95%, at r.t. and under stirring, was added *p*-fluorobenzaldehyde (0.134 ml, 1.27×10^{-3} mol) in 5 ml of EtOH 95%. Single needle-shaped and transparent crystals of Et-Hfbt (**1**, 80%), suitable for X-ray analysis, were grown by slow evaporation of the alcoholic solution of **1**. ^{1}H NMR (300 MHz, DMSO): δ 11.50 (1H, s, *NH*CS), 8.53 (1H, t, $J = 7.3$ Hz, *NH*CH_2CH_3), 8.08 (1H, s, CH=N), 7.85 (2H, m, H-2), 7.28 (2H, m, H-3), 3.61 (2H, quintet, $J = 7.3$ Hz, CH_2), 1.18 (3H, t, $J = 7.3$ Hz, CH_3). FTIR (KBr, cm^{-1}): ν (NH) 3366 (s), 3156 (ms); ν (CH) 3000 (mw); ν (C=C) 1602 (mw); ν (CN) 1550 (vs); ν (CS) 831 (m). MS (CI) m/z 226 (M + 1). *Anal.* Calc. for $C_{10}H_{12}N_3SF$: C, 53.32; H, 5.37; N, 18.66; S, 14.21. Found: C, 53.22; H, 5.30; N, 18.75; S, 14.30%.

The same procedure, as shown for compound **1**, was followed to obtain ligands Me-Hfbt (*p*-fluorobenzaldehyde N^4-methylthiosemicarbazone), allyl-Hfbt (*p*-fluorobenzaldehyde N^4-allylthiosemicarbazone), Ph-Hfbt (*p*-fluorobenzaldehyde N^4-phenylthiosemicarbazone), Me_2-Hfbt (*p*-fluorobenzaldehyde N^4,N^4-dimethylthiosemicarbazone) and MePh-Hfbt (*p*-fluorobenzaldehyde N^4-3-methylphenylthiosemicarbazone) [5].

2.2. Synthesis of the complexes **2**–**7**

2.2.1. [Ni(Et-fbt)$_2$] (**2**)

To a solution of Et-Hfbt (**1**) (0.017 g, 7.71×10^{-5} mol) in 10 ml of absolute EtOH, under stirring and reflux heating, $NiAc_2 \cdot 4H_2O$ (0.019 g, 7.71×10^{-5} mol) was added in a 1:1 molar ratio with respect to ligand **1**. Single needle-shaped blue crystals of [Ni(Et-fbt)$_2$] (**2**) were grown by slow evaporation of the alcoholic solution of **2**. ^{1}H NMR (300 MHz, DMSO): δ 8.27 (2H, dd, $J = 7.7$, 4.9 Hz, H-2), 7.62 (1H, bs, *NH*CH_2CH_3), 7.44 (1H, s, CH=N), 7.25 (2H, t, $J = 7.7$ Hz, H-3), 3.24 (2H, m, CH_2), 1.13 (3H, t, $J = 7.3$ Hz, CH_3). FTIR (KBr, cm^{-1}): ν (NH) 3439 (vs); ν (C=C) + ν (CN) 1596 (m); ν (CN) 1580 (m), 1530 (vs); ν (CS) 822 (mw). *Anal.* Calc. for $C_{20}H_{24}NiN_6F_2S_2$: C, 47.24; H, 4.76; N, 16.54; S, 12.59. Found: C, 47.14; H, 4.68; N, 16.66; S, 12.70%.

2.2.2. Ni(Me-fbt)$_2$] (**3**)

To a solution of Me-Hfbt (0.011 g, 5.44×10^{-5} mol) in 10 ml of EtOH 95%, under stirring and reflux heating, was added, in a 1:2 molar ratio with respect to the ligand, $NiAc_2 \cdot 4H_2O$ (0.007 g, 2.72×10^{-5} mol). Green crystals of [Ni(Me-fbt)$_2$] (**3**) were grown by slow evaporation of the alcoholic solution. ^{1}H NMR (300 MHz, DMSO): δ 8.31 (1H, bs, *NH*CH_3), 7.57 (2H, dd, $J = 7.15$, 5.6 Hz, H-2), 7.46 (1H, s, CH=N), 7.26 (2H, t,

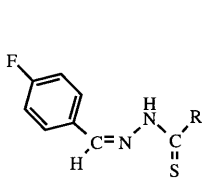

R	*Symbol*
NHEt	Et-Hfbt, [Ni(Et-fbt)$_2$] (**1**, **2**)
NHMe	[Ni(Me-fbt)$_2$] (**3**)
NHAllyl	[Ni(Allyl-fbt)$_2$] (**4**)
NHPh	[Ni(Ph-fbt)$_2$] (**5**)
NMe_2	[Ni(Me_2-fbt)$_2$](**6**)
NHPhMe	[Ni(MePh-fbt)$_2$] (**7**)

Fig. 1.

Table 1
Crystallographic data for ligand Et-Hfbt (**1**) and complex [Ni(Et-fbt)$_2$] (**2**) [a]

	Et-Hfbt (**1**)	[Ni(Et-fbt)$_2$] (**2**)
Formula	$C_{10}H_{12}N_3FS$	$C_{20}H_{24}NiN_6F_2S_2$
M	225.28	509.28
Crystal symmetry	monoclinic	monoclinic
Space group	$P2_1/c$	$P2_1/n$
Unit cell dimensions		
a (Å)	4.726(2)	11.206(6)
b (Å)	25.369(8)	14.186(9)
c (Å)	9.784(4)	14.241(9)
α (°)	90.0	90.0
β (°)	103.50(3)	95.19(7)
γ (°)	90.0	90.0
V (Å^3)	1140.6(8)	2255(2)
Z	4	4
D_{calc} (g cm^{-3})	1.31	1.50
F(000)	472	1056
μ (cm^{-1})	24.2	10.8
λ (Å)	1.54184	0.71069
Radiation	Cu Kα	Mo Kα
θ Range (°)	3–70	3–30
No. of unique reflections	1347	2531
R	0.053	0.036

[a] Data for compound **1**: Cu Kα radiation ($\lambda = 1.54184$ Å); Siemens-AED diffractometer, $T = 293 \pm 1$ K, $P = [\mathrm{Max}(F_o^2, 0) + 2F_c^2]/3$. Data for complex **2**: Mo Kα radiation ($\lambda = 0.71069$ Å); Philips diffractometer, $T = 293 \pm 1$ K, $P = [\mathrm{Max}(F_o^2, 0) + 2F_c^2]/3$.

$J = 7.15$ Hz, H-3), 2.83 (3H, d, $J = 4.6$ Hz, CH_3NH). FTIR (KBr, cm^{-1}): *v* (NH) 3432 (m), 3230 (m); *v* (CH) 3010 (m); *v* (C=C) 1604 (m); *v* (CN) 1597 (m); *v* (CS) 827 (m). *Anal*. Calc. for $C_{18}H_{18}NiN_6F_2S_2$: C, 45.18; H, 3.79; N, 17.58; S, 13.38. Found: C, 45.07; H, 3.70; N, 17.70; S, 13.49%.

2.2.3. [Ni(allyl-fbt)$_2$] (**4**)

To a solution of allyl-Hfbt (0.066 g, 2.78×10^{-4} mol) in 10 ml of EtOH 95%, under stirring and reflux heating, was added, in a 1:2 molar ratio with respect to the ligand, $NiAc_2 \cdot 4H_2O$ (0.034 g, 1.39×10^{-4} mol). Brown crystals of [Ni(allyl-fbt)$_2$] (**4**) were grown by slow evaporation of the alcoholic solution. ^{1}H NMR (300 MHz, DMSO): δ 8.28 (1H, t, $J = 1.8$ Hz, *NH*CH$_2$), 7.81 (2H, m, H-2), 7.47 (1H, s, CH=N), 7.24 (2H, m, H-3), 5.92 (1H, m, CH$_2$=*CH*–CH$_2$), 5.21 (1H, dd, $J = 16.0$, 2.0 Hz, *CH*$_2$=CH, H-β), 5.11 (1H, dd, $J = 8.0$, 2.0 Hz, *CH*$_2$=CH, H-α), 3.86 (2H, dd, $J = 6.0$, 1.8 Hz, CH–*CH*$_2$NH). FTIR (KBr, cm^{-1}): *v* (NH) 3429 (vs); *v* (CH) 3020 (ms); *v* (C=C) 1633 (m); *v* (CN) 1596 (m); *v* (CS) 823 (mw). *Anal*. Calc. for $C_{22}H_{22}NiN_6F_2S_2$: C, 49.81; H, 4.18; N, 15.85; S, 12.06. Found: C, 49.72; H, 4.10; N, 15.97; S, 12.17%.

2.2.4. [Ni(Ph-fbt)$_2$] (**5**)

To a solution of Ph-Hfbt (0.018 g, 6.70×10^{-5} mol) in 10 ml of EtOH 95%, under stirring and reflux heating, was added, in a 1:2 molar ratio with respect to the ligand, $NiAc_2 \cdot 4H_2O$ (0.008 g, 3.35×10^{-5} mol). Single needle-shaped yellow crystals of [Ni(Ph-fbt)$_2$] (**5**) were grown by slow evaporation of the alcoholic solution. ^{1}H NMR (300 MHz, DMSO): δ 9.78 (1H, s, *NH*Ph), 8.28 (2H, m, H-2), 7.77 (1H, s, CH=N), 7.55 (2H, m, H-3), 7.33 (2H, m, H *meta* phenyl), 7.25 (3H, m, H *ortho* phenyl + H *para* phenyl). FTIR (KBr, cm^{-1}): *v* (NH) 3414 (vs); *v* (CH) 2950 (s); *v* (C=C) 1624 (m); *v* (CN) 1596 (m); *v* (CS) 820 (w). *Anal*. Calc. for $C_{28}H_{22}NiN_6F_2S_2$: C, 55.81; H, 3.68; N, 13.96; S, 10.62. Found: C, 55.69; H, 3.59; N, 14.08; S, 10.73%.

2.2.5. [Ni(Me$_2$-fbt)$_2$] (**6**)

To a solution of Me$_2$-Hfbt (0.018 g, 8.00×10^{-5} mol) in 10 ml of EtOH 95%, under stirring and reflux heating, was added, in a 1:2 molar ratio with respect to the ligand, $NiAc_2 \cdot 4H_2O$ (0.010 g, 4.00×10^{-5} mol). Single needle-shaped brown crystals of [Ni(Me$_2$-fbt)$_2$] (**6**) were grown by slow evaporation of the alcoholic solution. ^{1}H NMR (300 MHz, DMSO): δ 8.24 (1H, s, CH=N), 7.45 (2H, m, H-2), 7.20 (2H, m, H-3), 3.29 and 3.16 (6H, 2s, 3H each, *CH*$_3$N). FTIR (KBr, cm^{-1}): *v* (NH) 3468 (ms, br); *v* (CH) 2925 (w); *v* (C=C) + *v* (CN) 1600 (m); *v* (CS) 826 (mw). *Anal*. Calc. for $C_{20}H_{22}NiN_6F_2S_2$: C, 47.42; H, 4.38; N, 16.60; S, 12.64. Found: C, 47.30; H, 4.29; N, 16.72; S, 12.71%.

2.2.6. [Ni(MePh-fbt)$_2$] (**7**)

To a solution of MePh-Hfbt (0.012 g, 4.18×10^{-5} mol) in 10 ml of EtOH 95%, under stirring and reflux heating, was added, in a 1:2 molar ratio with respect to the ligand, $NiAc_2 \cdot 4H_2O$ (0.005 g, 2.09×10^{-5} mol). Brown crystals of [Ni(MePh-fbt)$_2$] (**7**) were grown by slow evaporation of the alcoholic solution. ^{1}H NMR (300 MHz, DMSO): δ 9.70 (1H, s, *NH*Ph), 8.30 (2H, m, H-2), 7.77 (1H, s, CH=N), 7.51 (2H, m, H *ortho* phenyl + H *meta* phenyl), 7.25 (3H, m, H-3 + H *para* phenyl), 6.87 (1H, d, $J = 7.15$ Hz, H *ortho* phenyl), 2.29 (3H, s, CH$_3$). FTIR (KBr, cm^{-1}): *v* (NH) 3386 (vs); *v* (CH) 2930 (w); *v* (C=C) + *v* (CN) 1598 (m); *v* (CS) 831 (m). *Anal*. Calc. for $C_{30}H_{26}NiN_6F_2S_2$: C, 57.13; H, 4.16; N, 13.33; S, 10.15. Found: C, 57.00; H, 4.07; N, 13.45; S, 10.28%.

2.3. X-ray crystallography

Crystal data and details of structure refinement are given in Table 1. The single crystal diffraction measurements for compound **1** were carried out on a Siemens AED three circle diffractometer with the θ–2θ scan technique, using the Ni-filtered Cu Kα radiation ($\lambda = 1.54184$ Å). For complex **2** the intensity data were carried out on a Philips diffractometer using the Mo Kα radiation ($\lambda = 0.71069$ Å). Intensities were measured following a modified version [6] of the method of

Table 2
^{1}H NMR (300 MHz, DMSO) chemical shifts of compounds **1**–**7**

Compound	NHCS	NHR	CH=N	H-2	H-3
1	11.50 (1H, s)	8.53 (1H, t)	8.08 (1H, s)	7.85 (2H, m)	7.28 (2H, m)
2	–	7.62 (1H, bs)	7.44 (1H, s)	8.27 (2H, dd)	7.25 (2H, t)
3	–	8.31 (1H, bs)	7.46 (1H, s)	7.57 (2H, dd)	7.26 (2H, t)
4	–	8.28 (1H, t)	7.47 (1H, s)	7.81 (2H, m)	7.24 (2H, m)
5	–	9.78 (1H, s)	7.77 (1H, s)	8.28 (2H, m)	7.55 (2H, m)
6	–	–	8.24 (1H, s)	7.45 (2H, m)	7.20 (2H, m)
7	–	9.70 (1H, s)	7.77 (1H, s)	8.30 (2H, m)	7.25 (2H, m)

profile analysis by Lehmann and Larsen [7], and were corrected for Lorentz and polarization effects. The structures of all compounds were solved by direct methods using SIR-92 [8]. Refinements were carried out by full-matrix least-squares cycles using SHELXL-97 [9] for compounds **1** and **2**. The hydrogen atoms, located on a difference map, were refined for both products**.** Only in compound **1** were the hydrogen atoms of the ethyl group placed in calculated positions. Analytical expressions of neutral-atom scattering factors were employed according to the International Tables [10]. All calculations were performed on an ENCORE 91 computer at the Centro di Studio per la Strutturistica Diffrattometrica del C.N.R. (Parma). Molecular geometry calculations were carried out by using the computer program PARST [11] and the structure drawings by using the ORTEP [12] and PLUTO [13] programs.

3. Results and discussion

3.1. NMR spectra

The ^{1}H NMR spectrum of compound Et-Hfbt **1** (300 MHz, DMSO) shows, at r.t., the NHCS singlet, very deshielded, at 11.50 ppm, the $NHCH_2CH_3$ triplet at 8.53 ppm, and the signal of the proton on the C=N double bond at 8.08 ppm. The aromatic protons are found in the range 7.85–7.28 ppm (Table 2).

The complex [Ni(Et-fbt)$_2$] (**2**) (300 MHz, DMSO), obtained from ligand **1** and $NiAc_2{\cdot}4H_2O$, exhibits the aromatic protons at 8.27 and 7.25 ppm, the NH signal at 7.62 ppm, and the proton on the C=N double bond at 7.44 ppm (Table 2). The substituted NH proton (found at 8.53 ppm in the free ligand **1**) is shielded with respect to compound **1**, as well as the proton on the C=N double bond (observed at 8.08 ppm in the free ligand **1**): probably these two groups fall inside the benzene shielding cone (Table 2).

On the contrary, the H-2 aromatic hydrogens result deshielded at 8.27 ppm in complex **2** (at 7.85 ppm in compound **1**), presumably being outside the shielding cone, while the H-3 protons do not show any significant changes in the chemical shift (7.25 versus 7.28 ppm in **1**). A behaviour similar to compound **2** has also been detected for the nickel complexes **3**–**7**.

3.2. IR spectra

The IR spectra of compound **1** shows two bands in the frequency range 4000–3000 cm^{-1}, one due to the stretching frequencies ν (NH_2) (at 3366 cm^{-1}) and the other one to the hydrazine NH (at 3156 cm^{-1}, Table 3). On this basis, we have hypothesized that product **1** would form, during the crystallization, coupled dimers stabilized by an intramolecular hydrogen bond ($N–H_{terminal}\cdots N_{iminic}$), as found by the X-ray analysis.

A different spectral behaviour was observed for compound **2** [Ni(Et-fbt)$_2$]. In fact, when ligand **1** is coordinated via N, S to the nickel atom, just one strong band ν (NH) occurs at 3439 cm^{-1}, together with a separation of 50 cm^{-1} of the ν (C=N) (at 1580 and at 1530 cm^{-1}), and a 9 cm^{-1} shift of the band ν (CS) appearing at 822 cm^{-1} (Table 3).

This means that ligand **1** deprotonated before coordinating the metal, thus determining a square planar surrounding. As can be easily seen from Table 3, the IR spectra of products **3**, **4**, **5**, **6** and **7** are analogous to that of complex [Ni(Et-fbt)$_2$] (**2**). In this way, and in agreement with the microanalyses data, we have hypothesized that these ligands, after deprotonation and coordination with the metal, should present a S_2N_2 square planar configuration.

Table 3
IR (cm^{-1}) principal bands for compounds **1**–**7**

Compound	ν(NH)	ν(CN)	ν(CS)
1	3366(s), 3156(ms)	1550(vs)	831(m)
2	3439(vs), –	1580(vs)	822(mw)
3	3432(m), 3230(m), –	1597(m)	827(m)
4	3429(vs), –	1596(m)	823(mw)
5	3414(vs), –	1596(m)	820(w)
6	3468(ms,br), –	1600(m)	826(mw)
7	3386(vs), –	1598(m)	831(m)

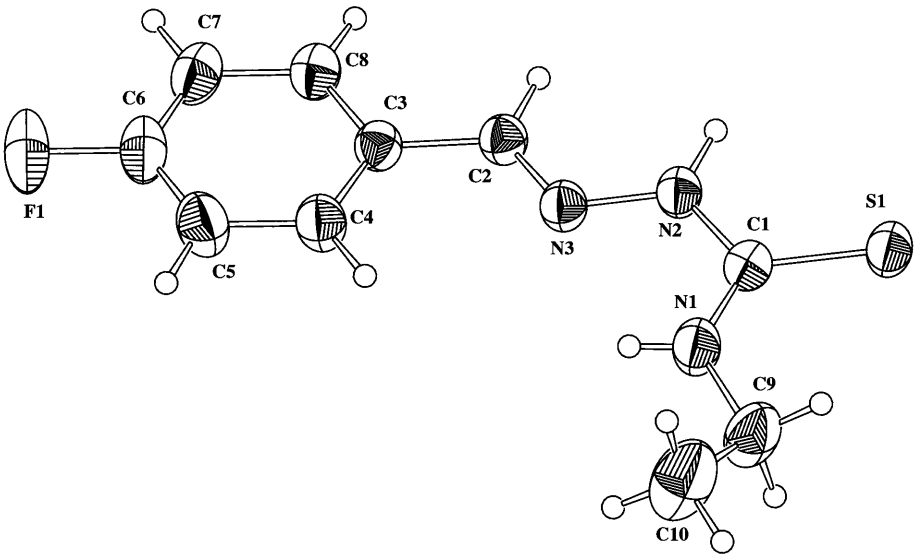

Fig. 2. Perspective view of Et-Hfbt (**1**) with thermal ellipsoids at the 50% probability level.

3.3. X-ray crystallography

The structures of *p*-fluorobenzaldehyde N^4-ethylthiosemicarbazone Et-Hfbt (**1**) has been determined. In Fig. 2 an ORTEP [12] drawing of the molecule of compound **1** is shown. The molecular conformation of the sulfur atom and the hydrazine nitrogen N3 (crystallographic numbering) is *trans* with respect to the C1–N2 bond, and the packing is determined by the presence of the strong intramolecular hydrogen bond N1–H···N3 = 2.607(4) Å. The angle between the thiourea group and the aromatic ring is small (6.4(2)°), and therefore the whole molecule is fairly planar. The bond distances of the benzene ring and the thiosemicarbazonic chain remain analogous to those found in similar fluorurated compounds (Table 4) [14]. Pairs of intermolecular hydrogen bonds N2–H···S($1-x$, $-y$, $1-z$) = 3.394(3) Å promote the dimers formation, linked by weak hydrogen bonds C10–H10···F($x+2$, $1/2-y$, $z+1/2$) = 3.523(8) Å, with an angle C10–H10···F = 155° and H···F = 2.630 Å [15,16]. Weak interactions C2···C8($1+x$, y, z) (3.556(6) Å) arise along the x axis that is particularly short.

Also, a complex derived from the reaction of ligand **1** with $NiAc_2$, the bis(*p*-fluorobenzaldehyde ethylthiosemicarbazonato)nickel(II) ([Ni(Et-fbt)$_2$], **2**) has been structurally characterized (Fig. 3). Differently from the similar previously synthesized complex [Ni(fbt)$_2$] [5], the nickel atom is not placed in a special position, and two independent ligand molecules are present. The coordination results in a square planar configuration slightly twisted towards a tetrahedron, involving the sulfur and the hydrazine nitrogen atoms of the two ligands in a *trans* configuration, with the Ni atom displaced by 0.06 Å from the coordination plane. The monodeprotonated ligand still behaves as bidentate with the sulfur and the nitrogen atoms in *cis* position with respect to the C–N bonds, and the right conformation for the complexation can be obtained from a 180° rotation (with respect to the free ligand **1**) around the C1–N2 and the C11–N5 bonds, respectively, for the two ligand molecules. The bond distances Ni–S1 2.172(2) Å, Ni–S2 2.171(2) Å, Ni–N3 1.927(3) Å and Ni–N6 1.926(3) Å (Table 4)

Table 4
Comparison between bond distances (Å) and angles (°) for **1**, **2** and [Ni(fbt)$_2$] [5]

	Et-Hfbt (**1**)	[Ni(Et-fbt)$_2$] (**2**)		[Ni(fbt)$_2$] [5]
Bond lengths				
Ni–S1		2.172(2)	2.171(2) [a]	2.2075(12)
Ni–N3		1.927(3)	1.926(3) [a]	1.934(4)
S1–C1	1.679(4)	1.727(4)	1.722(4) [a]	1.750(4)
F1–C6	1.356(5)	1.363(5)	1.360(5) [a]	1.370(6)
N1–C1	1.320(5)	1.348(5)	1.341(5) [a]	1.363(5)
N1–C9	1.447(6)	1.452(6)	1.438(6) [a]	
N2–N3	1.370(4)	1.381(4)	1.388(4) [a]	1.409(4)
N2–C1	1.351(4)	1.302(4)	1.311(5) [a]	1.324(5)
N3–C2	1.273(4)	1.299(5)	1.307(5) [a]	1.312(5)
C2–C3	1.466(5)	1.455(5)	1.462(5) [a]	1.480(6)
C3–C4	1.384(5)	1.396(5)	1.380(5) [a]	1.406(6)
C3–C8	1.393(5)	1.385(5)	1.395(5) [a]	1.418(6)
C4–C5	1.382(6)	1.367(6)	1.382(6) [a]	1.403(7)
C5–C6	1.372(7)	1.368(6)	1.362(6) [a]	1.390(6)
C6–C7	1.356(7)	1.342(7)	1.344(7) [a]	1.377(6)
C7–C8	1.383(6)	1.383(6)	1.372(7) [a]	1.400(7)
C9–C10	1.416(8)	1.493(7)	1.501(7) [a]	
Bond angles				
S1–Ni–N3		85.35(11)	85.57(11) [a]	84.90(10)
N3–Ni–S2		94.08(10)	94.90(10) [a]	95.10(10)

[a] Corresponding values found for the second independent molecule of complex **2**. The atomic numbering is shown in Fig. 3.

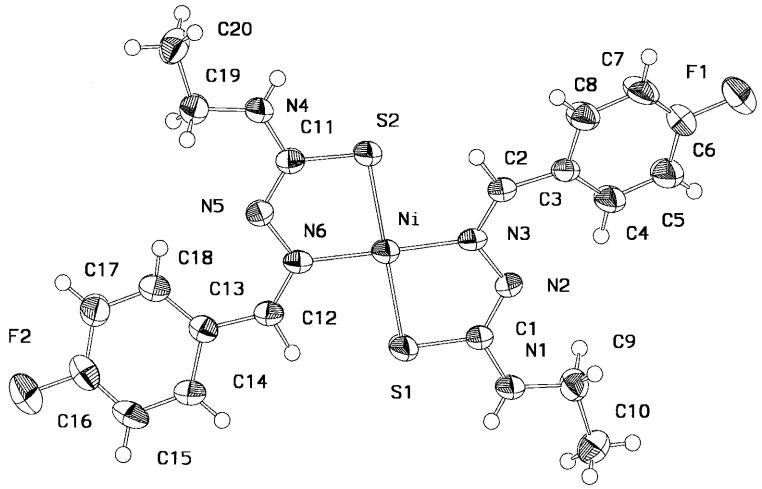

Fig. 3. Perspective view of complex [Ni(Et-fbt)$_2$] (**2**) with thermal ellipsoids at the 50% probability level.

agree with the correspondent values found for square planar and slightly twisted coordinations [4d,14]. The chelation ring NiN3N2C1S1 presents an *envelope* conformation (*puckering* parameters: $q_2 = 0.130(2)$ Å, $\varphi_2 = -176(1)°$), while the conformation of the other ring NiN6N5C11S2 is intermediate between *twist* and *envelope* ($q_2 = 0.085(2)$ Å, $\varphi_2 = -11(1)°$) [17], showing an interplanar angle of 4.7°. In this case the deprotonation of the nitrogen atoms N2 and N5 produces a charge delocalization in the C2N3N2C1N1S1 and C12N6N5C11N4S2 systems (Table 4), but less strong than in complex [Ni(fbt)$_2$] [5]. In fact the distances S1–C1 = 1.727(4) Å and S2–C11 = 1.722(4) Å (thiolic form), C1–N2 = 1.302(4) Å and C11–N5 = 1.311(5) Å, C2–N3 = 1.299(5) Å and C12–N6 = 1.307(5) Å were detected for complex **2**, while the corresponding values for the free ligand Et-Hfbt (**1**) resulted in S1–C1 = 1.679(4) Å (thionic form), C1–N2 = 1.351(4) Å and C2–N3 = 1.273(4) Å (due to a major localization of the double bond). The angle between the thiourea group and the aromatic ring is 17.5(1)° and 15.0(1)°, respectively, for the two ligand molecules: both values are larger than that observed in the free ligand (6.4(2)°), which is almost planar. The packing is determined by hydrogen bonds between the aminic nitrogen atoms and the fluorine atoms (N1···F1($x+1$, y, z) = 3.267(4) Å, N1–H···F1 168(3)°, N4···F2($x-1$, y, z) = 3.329(4) Å, N4–H···F2 164(3)°), that form chains of complexes along the x axis, and by weak non-bonding interactions (N3···N4($-x$, $-y$, $-z$) = 3.472(5) Å, N5···C2($-x$, $-y$, $-z$) = 3.378(5) Å, C6···C16($x-1$, $1/2-y$, $1/2+z$) = 3.486(6) Å, C8···C18($-x$, $-y$, $-z$) = 3.528(6) Å, C11···N3($-x$, $-y$, $-z$) = 3.572(5) Å, C15···C5($x+1$, $1/2-y$, $z-1/2$) = 3.595(7) Å).

4. Supplementary material

Crystallographic data for the structures reported in this paper have been deposited with the Cambridge Crystallographic Data Centre, CCDC no. 145284 for Et-Hfbt (**1**) and CCDC no. 145285 for [Ni(Et-fbt)$_2$] (**2**). Copies of this information may be obtained free of charge from the Director, CCDC, 12 Union Road, Cambridge, CB2 1EZ, UK (fax: +44-1223-336-033; e-mail: deposit@ccdc.cam.ac.uk or http://www.ccdc.cam.ac.uk).

Acknowledgements

This work was supported by Italian MURST (COFIN 98) in the frame of the Project 'Pharmacological and Diagnostic Properties of Metal Complexes' (Coordinator Professor G. Natile). The authors acknowledge the Centro Interfacoltà di Misure 'Giuseppe Casnati' dell'Università di Parma for NMR and MS instrumental facilities, and D. Belletti, A. Cantoni and G. Pasquinelli for their valuable technical assistance.

References

[1] M. Belicchi Ferrari, G. Gasparri Fava, E. Leporati, G. Pelosi, R. Rossi, P. Tarasconi, R. Albertini, A. Bonati, P. Lunghi, S. Pinelli, J. Inorg. Biochem. 70 (1998) 145.
[2] A.G. Eliopoulos, D.J. Kerr, J. Herod, L. Hodgkins, S. Krajewsk, J.C. Reed, L.S. Young, Oncogene 11 (1995) 1217.
[3] M.A. Halcrow, G. Cristou, Chem. Rev. 94 (1994) 2421.
[4] (a) M. Laing, P. Sommerville, P.A. Alsop, J. Chem. Soc. A (1971) 1247. (b) R.G. Hazell, Acta Chem. Scand. Ser. A 30 (1976) 322. (c) V.G. Puranik, S.S. Tavale, T.N.G. Row, P.

Umpathy, A.P. Budhkar, Acta Crystallogr., Sect. C (Cr. Str. Comm.) 43 (1987) 2303. (d) N.T. Akinchan, R. Akinchan, U.J. Ibok, L.P. Battaglia, A.B. Corradi, P. Drozdzewski, J. Crystallogr. Spectrosc. Res. 22 (1992) 741. (e) R. Alonso, E. Bermejo, A. Castineiras, T. Perez, R. Carballo, Z. Anorg. Allg. Chem. 623 (1997) 818.

[5] M. Belicchi Ferrari, S. Capacchi, G. Reffo, G. Pelosi, P. Tarasconi, R. Albertini, S. Pinelli, P. Lunghi, J. Inorg. Biochem. 81 (2000) 89.

[6] D. Belletti, A. Cantoni, G. Pasquinelli, Gestione on line di diffrattometro a cristallo singolo Siemens AED con sistema IBM PS 2/30, Internal Report 1/88, Centro di studio per la Strutturistica diffrattometrica del CNR, 1988.

[7] M.S. Lehmann, F.K. Larsen, Acta Crystallogr., Sect. A 30 (1974) 580.

[8] A. Altomare, G. Cascarano, C. Giacovazzo, A. Guagliardi, M.C. Burla, G. Polidori, M. Camalli, SIR-92, J. Appl. Crystallogr. 27 (1994) 435.

[9] G. Sheldrick, SHELXL-97, University of Göttingen, Germany, 1997.

[10] International Tables for X-Ray Crystallography, vol. 4, Kynoch Press, Birmingham, 1975.

[11] M. Nardelli, Comput. Chem. 7 (1983) 95.

[12] C.K. Johnson, ORTEP Report ORNL 3794, Oak Ridge National Laboratory, Tennessee, 1965.

[13] W.D.S. Motherwell, PLUTO, University Chemical Laboratory Cambridge, 1976.

[14] F.H. Allen, O. Kennard, Chemical Design Automation News 8 (1993) 1 & 31.

[15] V. Bertolasi, V. Ferretti, G. Gilli, P.A. Borea, J. Chem. Soc., Perkin Trans. 2 (1990) 283.

[16] R. Taylor, O. Kennard, J. Am. Chem. Soc. 104 (1982) 5063.

[17] D. Cremer, J.A. Pople, J. Am. Chem. Soc. 97 (1975) 1354.